Original Research Article

Nonlinear Radial Consolidation Analysis of Vertical Drains Foundation under Cyclic Loadings

Abstract: Aiming at the storage facilities built in soft soil areas, this paper analyzes the influence of cyclic loading on consolidation during use. Firstly, the nonlinear compressibility and permeability of soil are introduced, the well resistance and three kinds of radial permeability coefficient modes are considered, the corresponding governing equations are obtained, and the corresponding analytical solution is obtained by the separation of variables method. Then, the corresponding solution under the action of trapezoidal and triangular cyclic loading is obtained. The rationality of the solution in this paper is proved by the degradation verification. Finally, the settlement of storage facilities during the use period is predicted by example analysis. The results show that the ratio of soil compression index to permeability index (C_c/C_k) and the radial permeability coefficient model have no significant influence on the average degree of consolidation. The load-related intermittent parameter β, the loading parameter α, and the parameter N_σ have a great influence on the average consolidation degree. The smaller the three parameters are, the more energy the load generates at the same time, and the greater the corresponding average degree of consolidation.
Keywords: consolidation, nonlinearity, vertical drain foundation, well resistance, cyclic loading

1、INTRODUCTION

Many storage facilities have been built in the soft soil areas of various countries to store food, oil, and liquefied natural gas resources. Storage facilities often experience repeated loading and unloading in the use stage, which can be regarded as low-frequency cyclic loading [1]. It is necessary to discuss the consolidation behavior of the foundation under cyclic loading due to the repeated loading and unloading in the use stage.

Baligh and Levadoux [2] and Juran and Bemardet [3] simulated cyclic loading in the consolidometer and pointed out that the excess pore water pressure cannot be completely dissipated under cyclic loading. Then, Favaretti and Soranzo [4,5] applied the above test method to the actual working conditions to predict the silo settlement under triangular cyclic loading. Subsequently, Rahal and Vuez [6-8] pointed out that in the use of silos, the upper load was not a dynamic loading, and it could be approximated as a sinusoidal cyclic loading. By comparing the measured settlement measurement results with the theoretical value, it was found that the two had a good consistency. Guan et al. [1] pointed out that the cyclic load can be divided into high frequency, medium frequency, and low-frequency cyclic load, considering the consolidation behavior of soft soil under different forms of low frequency trapezoidal cyclic load. Xie et al. [9,10] considered the nonlinear change of soil compressibility and obtained the one-dimensional nonlinear consolidation solution of single-layer soil foundation under trapezoidal cyclic loading. Razouki et al. [11] gave the one-dimensional consolidation differential equation under haversine cyclic loading and pointed out that the number of cycles required for the average degree of consolidation to reach a stable state increased with the decrease of the dimensionless time factor. Shi et al. [12] pointed out that from the measured settlement, the foundation settlement and excess pore water pressure also fluctuated when the storage facilities were used. Cheng et al. [13] used the

Haversine cyclic loading to simulate the traffic loading and analyzed the influence of factors such as the stopping period of cyclic load and load frequency on the consolidation. Indraratna et al. [14,15] used cyclic triaxial test to study the effectiveness of prefabricated vertical drains in improving the stability of soft soil under cyclic loading, and the results showed that the excess pore water pressure generated during cyclic loading could be effectively reduced under drainage conditions. Razouki [16] points out that the number of cycles required for the average degree of consolidation to reach a stable state increases with the increase of frequency, and the increase of drainage plate spacing also slows down the consolidation process. Based on the assumption of equal strain, Kim et al. [17] derived the analytical solution of shaft foundation consolidation under cyclic loading considering the nonlinear compressibility and permeability of soil. Jiang et al. [18,19] considered the nonlinear compressibility and permeability of soil, deduced the nonlinear consolidation control equation considering the variation of permeability coefficient and well resistance in smearing area under instantaneous load, and obtained the solution of the control equation.

At present, researchers have made many discussions on the consolidation of soft soil foundation under cyclic loading, but the consolidation of shaft foundation under cyclic loading is still less considered. Because of the proposed engineering background, the load during the use of storage facilities is considered as a low-frequency cyclic load with the constant loading. the nonlinear compressibility and permeability of soil are introduced, and the well resistance and three radial permeability coefficients are considered. The corresponding solutions are obtained, and the influence of cyclic load on consolidation is analyzed.

2、BASIC ASSUMPTIONS, OBJECTIVES, EQUATIONS, AND SOLUTIONS

In Figure 1, the radial permeability coefficient of smeared area and undisturbed area is expressed as $k_r(r)$, r and z represent radial and vertical coordinates respectively. q denotes the cyclic loading varying with time. The calculated thickness is H. The vertical permeability coefficient of soil is k_v. The corresponding permeability coefficients of the vertical drain, smear zone and unsmeared zone are k_w, k_s and k_h, and the corresponding radii are r_w, r_s and r_e.

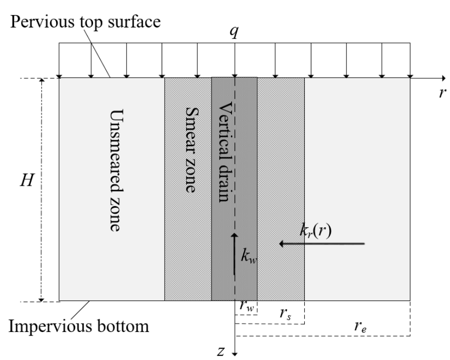

Fig.1 Calculation model for vertical drain

2.1 DERIVATION OF CONSOLIDATION EQUATION

According to the derivation process, the following assumptions are made : (1) the equal strain assumption is established, the loading and settlement occur only in the vertical direction, and there is no lateral deformation in the shaft foundation, and the vertical deformation at any depth is the same; (2) Only radial flow of soil is considered, and flow in soil and vertical drain conforms to Darcy's law; (3) Except for the permeability coefficient, the other properties of the soil in the shaft and smearing area are the same as those in the undisturbed area; (4) Assuming that the loading is applied instantaneously; (5) At any depth, the amount of water flowing from the soil into the shaft is equal to the increment of water flowing upward in the shaft; (6) Considering the nonlinear changes of soil compressibility and permeability, the void ratio has the following relationship with effective stress and permeability coefficient :

$$e = e_0 - C_c \lg(\sigma'/\sigma'_0) \quad (1)$$

$$e = e_0 + C_k \lg(k_h/k_{h0}) \quad (2)$$

Where e and e_0 are the void ratio at any moment and the initial moment, respectively; σ' and σ'_0 are the effective stress at any moment and the initial effective stress, respectively; k_h and k_{h0} are the radial permeability coefficients of the soil at any moment and the initial moment, respectively; C_c and C_k are the compression index and the permeability index, respectively.

Assuming that the radial permeability coefficient $k_r(r)$ varies with the radial distance away from the vertical drain:

$$k_\mathrm{r}(r) = k_\mathrm{h} f(r) \quad (3)$$

where $f(r)$ is the variation function of the permeability coefficient.

Based on the above assumptions, the radial consolidation control equation of vertical drain foundation [20]:

$$\frac{k_r(r)}{\gamma_w}\frac{1}{r}\frac{\partial}{\partial r}\left(r\frac{\partial u_r}{\partial r}\right) = -\frac{\partial \varepsilon_v}{\partial t}, r_w \le r \le r_e \quad (4)$$

According to assumption (5), the flow continuity equation is obtained :

$$2\pi r_\mathrm{w}\frac{k_\mathrm{s}}{\gamma_\mathrm{w}}\frac{\partial u_\mathrm{r}}{\partial r}\bigg|_{r=r_\mathrm{w}} = -\pi r_\mathrm{w}^2\frac{1}{\gamma_\mathrm{w}}\frac{\partial}{\partial z}\left(k_\mathrm{w}\frac{\partial u_\mathrm{w}}{\partial z}\right) \quad (5)$$

Where u_w is the average excess pore water pressure in the vertical drain.

The expression of average excess pore water pressure is :

$$\bar{u}_r = \frac{1}{\pi\left(r_\mathrm{e}^2 - r_\mathrm{w}^2\right)}\int_{r_\mathrm{w}}^{r_\mathrm{e}} 2\pi r u_r \mathrm{d}r \quad (6)$$

The boundary conditions are:

(1) Continuity of pore water pressure at $r = r_w, u_r = u_w$ (7.1)

(2) Impermeable cylindrical surface at $r = r_e, \frac{\partial u_r}{\partial r} = 0$ (7.2)

(3) At the top of the clay layer $z = 0, u_w = 0$ (7.3)

(4) For the impervious bottom $z = H, \frac{\partial u_\mathrm{w}}{\partial z} = 0$ (7.4)

(5) For the impervious bottom $t = 0, \bar{u}_r = q(t = 0)$ (7.5)

Integrating both the left and right ends of Eq.(4) over r and using the boundary condition (7.2):

$$\frac{\partial u_r}{\partial r} = \frac{\gamma_w}{2k_h}\frac{1}{f(r)}\left(\frac{r_e^2}{r} - r\right)\frac{\partial \varepsilon_v}{\partial t} \quad (8)$$

Then integrating both the left and right ends of Eq.(8) simultaneously over r and using the boundary condition (7.1):

$$u_r = \frac{\gamma_w}{2k_h}\frac{1}{f(r)}\frac{\partial \varepsilon_v}{\partial t}[r_e^2 \overline{B}(r) - \overline{C}(r)] + u_w \tag{9}$$

Where $\overline{B}(r) = \int_{r_w}^{r} \frac{1}{\xi f(\xi)} d\xi$, $\overline{C}(r) = \int_{r_w}^{r} \frac{\xi}{f(\xi)} d\xi$

Substituting Eq.(9) into Eq.(6), the average excess pore water pressure expression is obtained :

$$\overline{u}_r = \frac{\gamma_w r_e^2}{2k_h} F_c \frac{\partial \varepsilon_v}{\partial t} + u_w \tag{10}$$

Where $F_c = \frac{2(r_e^2 \overline{\overline{B}} - \overline{\overline{C}})}{r_e^2 (r_e^2 - r_w^2)}$, $\overline{\overline{B}} = \int_{r_w}^{r_e} r\overline{B}(r)dr$, $\overline{\overline{C}} = \int_{r_w}^{r_e} r\overline{C}(r)dr$ 。

When r=r_w, $k_r(r)$=k_s. According to Eq.(8)

$$\left.\frac{\partial u_r}{\partial r}\right|_{r=r_w} = \frac{\gamma_w r_w}{2k_s}(n^2-1)\frac{\partial \varepsilon_v}{\partial t} \tag{11}$$

Substitute Eq.(11) into Eq.(5):

$$\frac{\partial^2 u_w}{\partial z^2} = -\frac{\gamma_w}{k_w}(n^2-1)\frac{\partial \varepsilon_v}{\partial t} \tag{12}$$

Where $\frac{\partial \varepsilon_v}{\partial t} = m_v \frac{\partial \sigma'}{\partial t} = m_v \frac{\partial \sigma'}{\partial T_h}\frac{\partial T_h}{\partial t} = \frac{k_{h0}}{4r_e^2 \gamma_w}\frac{\sigma_0'}{\sigma'}(\frac{\partial q(T_h)}{\partial T_h} - \frac{\partial \overline{u}_r}{\partial T_h})$ (13)

In Eq.(13), m_v is defined as:

$$\begin{aligned} m_v &= -\frac{1}{1+e_0}\frac{\partial e}{\partial \sigma'} = m_{v0}(\frac{\sigma_0'}{\sigma'}) \\ m_{v0} &= \frac{C_c}{(1+e_0)\sigma_0' \ln 10} \end{aligned} \tag{14}$$

Substitute Eq.(13) into Eq.(10):

$$\frac{\partial \overline{u}_r}{\partial T_h} = \frac{\partial q}{\partial T_h} - \frac{8k_h}{F_c k_{h0}}\frac{\sigma'}{\sigma_0'}(\overline{u}_r - u_w) \tag{15}$$

Substitute Eq.(10) into Eq.(12):

$$\frac{\partial^2 u_w}{\partial z^2} = -\frac{2k_h(n^2-1)}{k_w r_e^2 F_c}(\overline{u}_r - u_w) \tag{16}$$

Substitute Eq.(1) into Eq.(15):

$$\frac{\partial \overline{u}_r}{\partial T_h} = \frac{\partial q}{\partial T_h} - \frac{8}{F_c}(\frac{\sigma'}{\sigma_0'})^{1-(C_c/C_k)}(\overline{u}_r - u_w) \tag{17}$$

Let $\lambda = (8/F_c)(\sigma'/\sigma_0')^{1-(C_c/C_k)}$, Then Eq.(17) becomes

$$\frac{\partial \bar{u}_r}{\partial T_h} = \frac{\partial q}{\partial T_h} - \lambda(\bar{u}_r - u_w) \tag{18}$$

Substitute Eq.(1) into Eq.(16):

$$\frac{\partial^2 u_w}{\partial z^2} = -\frac{2k_{h0}(n^2-1)}{k_w r_e^2 F_c}(\frac{\sigma'}{\sigma_0'})^{-(C_c/C_k)}(\bar{u}_r - u_w) \tag{19}$$

Let $\rho = (2k_{h0}(n^2-1)/k_w r_e^2 F_c)(\sigma'/\sigma_0')^{-(C_c/C_k)}$, Then Eq.(19) becomes:

$$\frac{\partial^2 u_w}{\partial z^2} = -\rho(\bar{u}_r - u_w) \tag{20}$$

According to the principle of effective stress $\sigma' = \sigma_0' + q - \bar{u}_r$, Then σ' changes from initial σ_0' to final $\sigma_0' + q_u$, Then take the average value $\frac{\sigma_0' + \sigma_0' + q_u}{2}$ as the value of σ' for solving, Let $N_\sigma = \left(\sigma_0' + q_u\right)/\sigma_0'$, then the corresponding λ and ρ become :

$$\begin{aligned} \lambda = \lambda' &= \frac{8}{F_c}(\frac{1+N_\sigma}{2})^{1-\frac{C_c}{C_k}} \\ \rho = \rho' &= \frac{2k_{h0}(n^2-1)}{k_w r_e^2 F_c}(\frac{1+N_\sigma}{2})^{-\frac{C_c}{C_k}} \end{aligned} \tag{21}$$

From Eq.(18), Eq.(20) and Eq.(21):

$$\frac{\partial^3 u_w}{\partial z^2 \partial T_h} + \lambda' \frac{\partial^2 u_w}{\partial z^2} - \rho' \frac{\partial u_w}{\partial T_h} = -\rho' \frac{\partial q}{\partial T_h} \tag{22}$$

Applying the separation of variables method to Eq.(22), the general solution is assumed to be

$$u_w = \sum_{m=1}^{\infty} T_m(T)\sin(\frac{M}{H}z) \tag{23}$$

Where $M = \frac{2m-1}{2}\pi$, (m=1,2,3…)。

From Eq.(23) and Eq.(20), the expression of average excess pore water pressure is :

$$\bar{u}_r = u_w - \frac{1}{\rho'}\frac{\partial^2 u_w}{\partial z^2} \tag{24}$$

Combined with boundary conditions (7.3), (7.4) and (7.5) and Eq.(22), the solution of Eq.(24) is :

$$\bar{u}_r = \sum_{m=1}^{\infty} \frac{2}{M} e^{-\beta_m T_h} \sin(\frac{M}{H}z)(q(0) + \int_0^{T_h} \frac{dq}{d\tau} e^{\beta_m \tau} d\tau) \tag{25}$$

Where $\beta_m = (\lambda'(\frac{M}{H})^2) \Big/ (\rho' + (\frac{M}{H})^2)$。

To consider the influence of vertical drain construction on the permeability coefficient of the surrounding soil, according to reference [21], three various modes of radial permeability coefficient are selected, as shown in Figure 2:

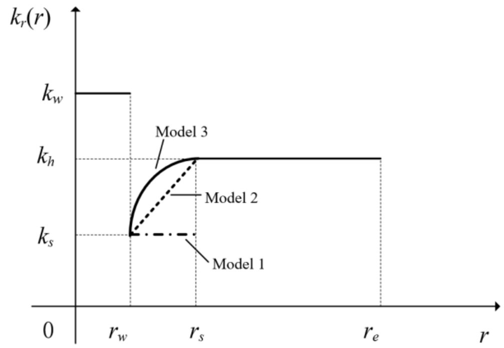

Fig.2 Three variation modes of radial permeability coefficient in the smear zone

Mode 1 shows that the radial permeability coefficient is k_s in the smear zone $r_w \le r \le r_s$, and k_h in the unsmeared zone $r_s \le r \le r_e$. The corresponding $f(r)$ and parameter F_c are :

$$f(r)=\begin{cases}1, & r_{\mathrm{w}} \le r \le r_{\mathrm{s}} \\ \alpha, & r_{\mathrm{s}} < r \le r_{\mathrm{e}}\end{cases} \tag{26}$$

$$F_{\mathrm{c}}=\left(\ln\frac{n}{s}+\alpha\ln s-\frac{3}{4}\right)\frac{n^2}{n^2-1}+\frac{s^2}{n^2-1}(1-\alpha)\times\left(1-\frac{s^2}{4n^2}\right)+\alpha\frac{1}{n^2-1}\left(1-\frac{1}{4n^2}\right) \tag{27}$$

Where $\alpha = k_h/k_s > 1$。

Mode 2 shows that the radial permeability coefficient of the soil in the smear zone decreases gradually to k_s with the decrease of r, and the radial permeability coefficient of the unsmeared zone is k_h. This mode is more realistic than mode 1, and the corresponding $f(r)$ and parameter F_c are :

$$f(r)=\begin{cases}\dfrac{r-r_{\mathrm{w}}}{r_{\mathrm{s}}-r_{\mathrm{w}}}(1-\alpha)+\alpha, & r_{\mathrm{w}} \le r \le r_{\mathrm{s}} \\ 1, & r_{\mathrm{s}} < r \le r_{\mathrm{e}}\end{cases} \tag{28}$$

$$\begin{aligned}F_c=\frac{n^2}{n^2-1}\Bigg\{&\frac{s-1}{\alpha s-1}\ln(\alpha s)-\frac{(s-1)^2}{n^2(1-\alpha)}+\frac{2(s-1)(\alpha s-1)}{n^2(1-\alpha)^2}\ln\frac{1}{\alpha}-\frac{2(s-1)}{n^4(1-\alpha)}\left(\frac{s^3-1}{3}-\frac{s^2-1}{2}\right)\\ &-\frac{(s-1)(\alpha s-1)}{n^4(1-\alpha)^2}\left[\frac{s^2-1}{2}-\frac{(s-1)(\alpha s-1)}{(1-\alpha)}+\frac{(\alpha s-1)^2}{(1-\alpha)^2}\ln\frac{1}{\alpha}\right]-\frac{\left(n^2-s^2\right)}{n^4}\frac{(1-s)^2}{(1-\alpha)}+\ln\frac{n}{s}-\frac{3}{4}+\frac{4n^2s^2-s^4}{4n^4}\Bigg\}\end{aligned} \tag{29}$$

Mode 3 shows that the radial permeability coefficient of soil in the smear zone presents a parabolic change with the increase of r, which increases from k_s to k_h. The radial permeability coefficient of soil in the unsmeared zone remains unchanged. This mode is the change of permeability coefficient measured by Indraratna et al. [22,23], and the corresponding $f(r)$ and parameter F_c are :

$$f(r)=\begin{cases}(1-\alpha)\left(a-b+c\dfrac{r}{r_{\mathrm{w}}}\right)\left(a+b-c\dfrac{r}{r_{\mathrm{w}}}\right), & r_{\mathrm{w}} \le r \le r_{\mathrm{s}} \\ 1, & r_{\mathrm{s}} < r \le r_{\mathrm{e}}\end{cases} \tag{30}$$

Where $a=\sqrt{1/(1-\alpha)}$, $b=s/(s-1)$, $c=1/(s-1)$, $d=\ln[(a+1)/(a-1)]$。

$$F_c=\left(a^2F_{c1}+n^2F_{c2}\right)\Big/\left(n^2-1\right) \tag{31}$$

Where

$$F_{c1}=\frac{1}{a^2-b^2}\left(s^2\ln s-\frac{s^2}{2}+\frac{1}{2}\right)-\frac{1}{\left(a^2-b^2\right)c^2}\left[-b+\frac{1}{2}+\left(\frac{a^2}{2}-b^2\right)\ln\alpha+\frac{abd}{2}\right]$$
$$+\frac{1}{n^2c^4}\left[-3b+\frac{1}{2}+\left(\frac{a^2}{2}+b^2\right)\ln\alpha+\frac{3abd}{2}\right] \tag{32}$$
$$F_{c2}=\ln\frac{n}{s}-\frac{3}{4}+\frac{s^2}{n^2}-\frac{s^4}{4n^4}+a^2\left(1-\frac{s^2}{n^2}\right)\left[\frac{1}{\left(a^2-b^2\right)}\left(\ln(s\sqrt{\alpha})-\frac{bd}{2a}\right)-\frac{1}{n^2c^2}\left(\ln\sqrt{\alpha}+\frac{bd}{2a}\right)\right]$$

The self-weight of storage facilities has always existed during use and the loading and unloading of storage facilities during use [12]. In this paper, the trapezoidal and triangular cyclic loading modes with constant loading are selected (shown in Fig.3). Each cycle of the cyclic load is t_0, N is a positive integer starting from 1, indicating the number of cycles, α is the loading parameter, and the time of loading and unloading is αt_0. If $\alpha = 0.5$, the trapezoidal cyclic loading becomes a triangular cyclic loading, and β represents the interval of the loading:

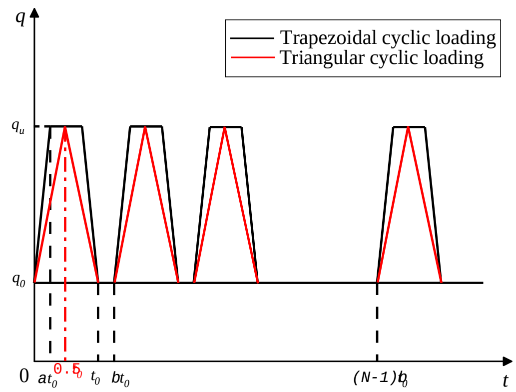

Fig.3 Schematic diagram of Trapezoidal and Triangular cyclic loadings

Define dimensionless parameters： $T_a=\frac{C_{h0}(N-1)\beta t_0}{4r_e^2}$ ， $T_d=\frac{C_{h0}\alpha t_0}{4r_e^2}$ ， $T_b=\frac{C_{h0}((N-1)\beta+1)t_0}{4r_e^2}$ ，

$T_h=\frac{C_{h0}t}{4r_e^2}$.

The expression of loading q is :

$$q=\begin{cases}\dfrac{q_u-q_0}{T_d}\left(T_h-T_a\right)+q_0, T_a\le T_h\le T_a+T_d\\ q_u, \qquad T_a+T_d\le T_h\le T_b-T_d\\ \dfrac{-\left(q_u-q_0\right)}{T_d}\left(T_h-T_b\right)+\alpha q_0, T_b-T_d\le T_h\le T_b\\ q_0, \qquad T_b\le T_h\le T_a\end{cases} \tag{33}$$

Substitute Eq.(33) into Eq.(25) to obtain the expression of average excess pore water pressure:

$$\bar{u}_r = \begin{cases} \sum_{m=1}^{\infty} \frac{2}{M} \exp\left(-\beta_m T_h\right)\left[q_0 + T_1\right] \sin\left(\frac{M}{H} z\right), T_a \le T_h \le T_a + T_d \\ \sum_{m=1}^{\infty} \frac{2}{M} \exp\left(-\beta_m T_h\right)\left[q_0 + T_2\right] \sin\left(\frac{M}{H} z\right), T_a + T_d \le T_h \le T_b - T_d \\ \sum_{m=1}^{\infty} \frac{2}{M} \exp\left(-\beta_m T_h\right)\left[q_0 + T_3\right] \sin\left(\frac{M}{H} z\right), T_b - T_d \le T_h \le T_b \\ \sum_{m=1}^{\infty} \frac{2}{M} \exp\left(-\beta_m T_h\right)\left[q_0 + T_4\right] \sin\left(\frac{M}{H} z\right), T_b \le T_h \le T_a \end{cases} \tag{34}$$

Where

$$\begin{aligned} &T_1 = \frac{q_u - q_0}{\beta_m T_d}\left[D_T(N-1) + D_{T1}\right], T_2 = \frac{q_u - q_0}{\beta_m T_d}\left[D_T(N-1) + D_{T2}\right], \\ &T_3 = \frac{q_u - q_0}{\beta_m T_d}\left[D_T(N-1) + D_{T2} - D_{T3}\right], T_4 = \frac{q_u - q_0}{\beta_m T_d}\left[D_T(N)\right], \\ &D_T = \sum_{N=1}^{n}\left(D_{T2} - D_{T4}\right), D_{T1} = \exp\left(\beta_m T_h\right) - \exp\left(\beta_m T_a\right), \\ &D_{T2} = \exp\left(\beta_m\left(T_a + T_d\right)\right) - \exp\left(\beta_m T_a\right), D_{T3} = \exp\left(\beta_m T_h\right) - \exp\left(\beta_m\left(T_b - T_d\right)\right), \\ &D_{T4} = \exp\left(\beta_m T_{\mathrm{b}}\right) - \exp\left(\beta_m\left(T_b - T_d\right)\right). \end{aligned} \tag{35}$$

The average consolidation degree U_p defined by excess pore water pressure is :

$$U_p = \left(\int_0^H \left(q - \bar{u}_r\right) dz \Big/ \int_0^H q_u dz\right) \tag{36}$$

The average consolidation degree U_s defined by deformation is :

$$U_s = \left(\int_0^H \varepsilon dz \Big/ \int_0^H \varepsilon_f dz\right) \tag{37}$$

Where $\varepsilon = \frac{e_0 - e}{1 + e_0} = \frac{c_c}{1 + e_0} \log\left(\frac{\sigma'}{\sigma'_0}\right)$ is the vertical strain at any time, $\varepsilon_f = \frac{e_f - e}{1 + e_0} = \frac{c_c}{1 + e_0} \log\left(\frac{\sigma'_f}{\sigma'_0}\right)$ is the vertical strain at any time, σ'_f is the final effective stress。

2.2 DEGRADATION VERIFICATION

Reference [18] gave the expression of average excess pore water pressure of vertical drain foundation considering the change of well resistance with time :

$$\bar{u}_{\mathrm{r}} = \sum_{m=1}^{\infty} \frac{2 q_{\mathrm{u}}}{M} \sin\left(\frac{Mz}{H}\right)\left(\frac{1 + F_{\mathrm{t}}}{1 + F_0}\right)^{\lambda_{\mathrm{a}}/\omega} \tag{38}$$

Where $F_{\mathrm{t}} = F_0 \exp(-\omega t)$, $F_0 = M^2 / \left(\rho_a H^2\right)$, conditions for constant well resistance at $\omega = 0$：

$$\lim_{\omega \to 0}\left(\frac{1 + F_{\mathrm{t}}}{1 + F_0}\right)^{\lambda_{\mathrm{a}}/\omega} = \exp\left(-\frac{\lambda_{\mathrm{a}} M^2}{\rho_{\mathrm{a}} H^2 + M^2} t\right) \tag{39}$$

Substitute Eq.(39) into Eq.(38) to obtain：

$$\bar{u}_{\mathrm{r}} = \sum_{m=1}^{\infty} \frac{2q_{\mathrm{u}}}{M} \sin\left(\frac{M}{H}z\right) \exp\left(-\frac{\lambda_{\mathrm{a}} M^2}{\rho_{\mathrm{a}} H^2 + M^2} t\right) \tag{40}$$

The expression of average excess pore water pressure is :

$$\bar{u}_r = \sum_{m=1}^{\infty} e^{-\beta_m T_h} \sin(\frac{M}{H}z) \frac{2}{M} (q(0) + \int_0^{T_h} \frac{dq}{d\tau} e^{\beta_m \tau} d\tau) \tag{25}$$

Where $\beta_m = (\lambda'(\frac{M}{H})^2) \Big/ (\rho' + (\frac{M}{H})^2)$. The loading on the right side of Eq.(25) changing with time is regarded as a constant loading q_u, get $\partial q / \partial T_h = 0$, substitute β_m into Eq.(25) to obtain :

$$\bar{u}_r = \sum_{m=1}^{\infty} \frac{2q_u}{M} \sin(\frac{M}{H}z) \exp(-\frac{\lambda' M^2}{\rho' H^2 + M^2} T_h) \tag{41}$$

It can be seen that Eq.(41) is consistent with Eq.(40). By studying the degradation of the solution and comparing it with the existing analytical solution, the rationality of the solution is verified.

3、CONSOLIDATION BEHAVIOR UNDER CYCLIC LOADINGS

This paper mainly analyzes the influence of C_c/C_k, different radial permeability coefficient modes, loading parameters α, intermittent parameters β and N_σ on consolidation. According to reference [24], the loading parameter α of trapezoidal cyclic load is 0.2, the interval parameter β of trapezoidal and triangular cyclic load is 1.2, and the calculated parameter is σ_0'=50kPa, q_u=75kPa, q_0=40kPa, C_c/C_k=1.5, r_e/r_w=15, r_s/r_w=4, k_h/k_s=5, k_w/k_{h0}=5000。

3.1 THE INFLUENCE OF C_C/C_K ON CONSOLIDATION

Figure 4 is the average consolidation curve corresponding to different C_c/C_k values under trapezoidal and triangular cyclic loadings. It can be seen that with the increase of C_c/C_k value, the time to reach the stable state under the same type of cyclic loading is prolonged, that is, the consolidation rate is reduced. Under different C_c/C_k values, U_s is higher than the corresponding U_p, indicating that the deformation rate is faster than the dissipation rate of pore pressure in the consolidation process. The average consolidation degree under trapezoidal cyclic loading is larger than that under triangular cyclic loading.

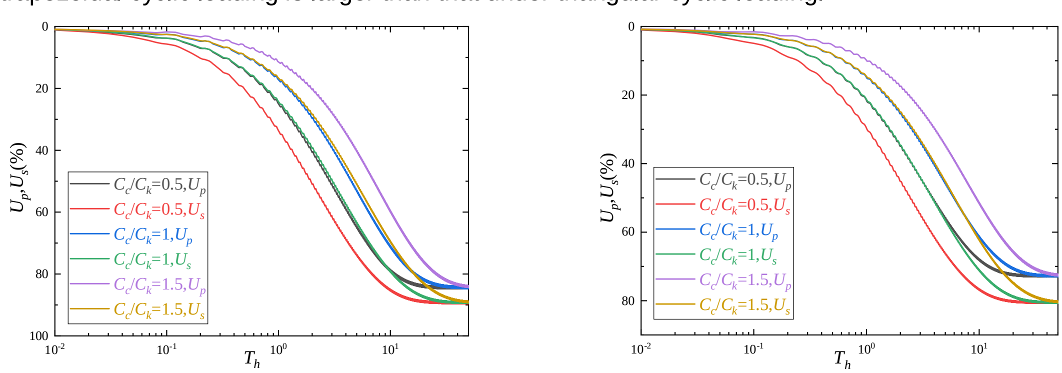

(a) Trapezoidal cyclic loading **(b) Triangular cyclic loading**

Fig.4 Average degree of consolidation at different values of C_c/C_k

3.2 THE INFLUENCE OF DIFFERENT MODES OF RADIAL PERMEABILITY COEFFICIENT ON

CONSOLIDATION

Figure 5 is the average consolidation curve of different radial permeability coefficient modes under trapezoidal and triangular cyclic loadings. From figure 2, it can be seen that the radial permeability coefficient corresponding to models 2 and 3 in the smear zone is greater than that of mode 1, but the difference between the two is small, so there is no big difference between the consolidation rate corresponding to mode 2 and 3, which is greater than the curve corresponding to mode 1.

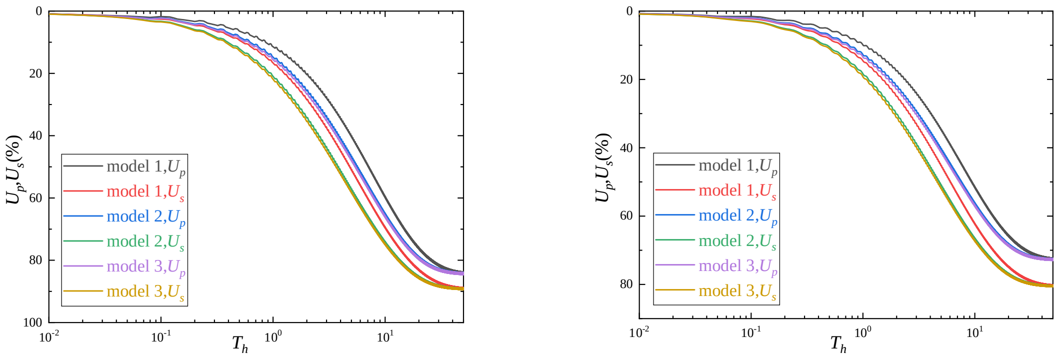

(a) Trapezoidal cyclic loading **(b) Triangular cyclic loading**

Fig.5 Average degree of consolidation corresponding to different modes of radial permeability coefficient

3.3 THE INFLUENCE OF INTERVAL PARAMETER *β* AND THE LOADING PARAMETER *α* ON CONSOLIDATION

Figure 6 and Figure 7 respectively show the influence of the interval parameter β and the loading parameter α on the average consolidation degree. It can be seen from Figure 6 that when the interval parameter $\beta = 1$, the cyclic loading has no interval, and the corresponding average consolidation degree is the largest. With the increase of parameter β, the average consolidation degree gradually decreases. It can be seen from Figure 7 that the smaller the loading parameter α is, the largest the average consolidation degree is. With the increase of parameter α, the time when the loading is at the maximum q_u decreases, resulting in the decrease of the average consolidation degree. It can be seen that the smaller the parameter β is, the shorter the loading interval is, the smaller the parameter α is, the faster the loading and unloading rate of the trapezoidal loading is, and the longer the duration of the dead load is, the more the energy generated by the load in the same time, resulting in the greater the average consolidation degree.

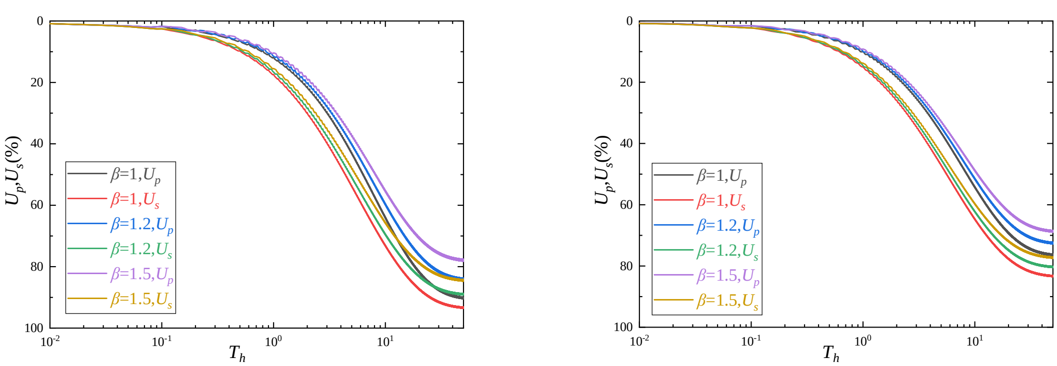

(a) Trapezoidal cyclic loading **(b) Triangular cyclic loading**

Fig.6 Effect of intermission parameter *β* on the average degree of consolidation

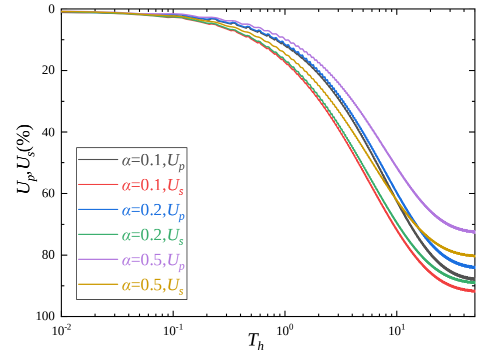

Fig.7 Effect of loading parameter *α* on the average degree of consolidation under Trapezoidal cyclic loading

3.4 THE INFLUENCE OF $N_σ$ ON CONSOLIDATION

Figure 8 shows the average consolidation curves corresponding to different $N_σ$ under trapezoidal and triangular cyclic loadings, respectively. Since the constant load is considered in this paper, it can be seen that the smaller the $N_σ$ is, the loading selected in this paper is closer to the constant loading, and the larger the corresponding average consolidation degree is.

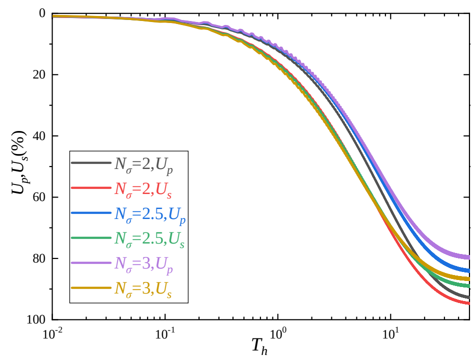

(a) Trapezoidal cyclic loading

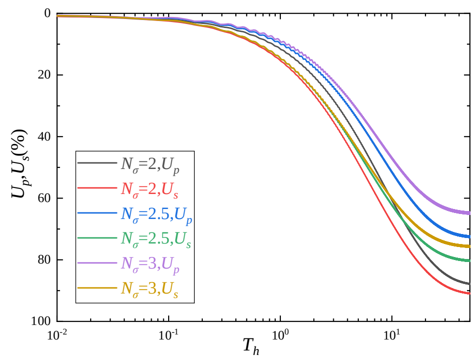

(b) Triangular cyclic loading

Fig.8 Average degree of consolidation at different values of $N_σ$

4. EXAMPLE ANALYSIS

Reference [24] referred to the construction of a 10000m³ storage tank on the soft soil foundation in a coastal area, in order to reduce the settlement of the foundation, the prefabricated vertical drains were arranged in advance in the foundation, which can be regarded as the working condition of the upper part of the shaft foundation under cyclic load in the use stage. According to Reference [24], in the use stage, the dimensionless time factor T_0 corresponding to the loading is 17.46, the maximum load is 165kPa, the intermittent period parameter $β$ is 1.2, the loading parameter $α$ is 0.33, and the setting depth of prefabricated vertical drains is 20 m. Other parameters such as the parameters used in the consolidation behavior analysis in this paper. The settlement curve of the tank within 2176 days (T_h=200) is shown in Fig.9.

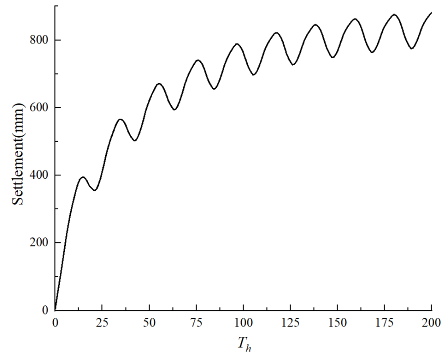

Fig.9 The method of this paper is used to predict the settlement of the use stage

The tank mentioned in Reference [24] only carried out one-time water-filling preloading. It can be seen from Fig.9 that consolidation settlement still occurred in the early use stage, and the maximum settlement of the shaft foundation was about 767 mm. In the steady state of settlement, the maximum settlement difference due to loading and unloading is 86.34 mm, approximately 109 days (T_h=10), the daily settlement is about 0.8mm. The maximum settlement difference can be used as the reference value of the tank design stage to ensure the safety of the tank in the use stage.

5 CONCLUSIONS

In this paper, the nonlinear consolidation solution of the vertical drain foundation considering constant well resistance and radial permeability coefficient variation under trapezoidal and triangular cyclic loadings is derived. The correctness and rationality of the solution in this paper are verified by degradation verification and example analysis, and the following conclusions are obtained:

(1) The analysis shows that the average consolidation degree under cyclic loadings is not 100 %, indicating that the excess pore water pressure in the soil cannot be completely dissipated. The final value of the average consolidation degree is independent of the C_c/C_k value and the radial permeability coefficient model, and these two parameters mainly affect the time when the average consolidation degree reaches a stable state. The smaller the C_c/C_k value, the shorter the time for the average degree of consolidation to reach a stable state, and the greater the radial permeability coefficient in the smear area, the faster the time for the average degree of consolidation to reach a stable state.

(2) Load-related parameters β, α and N_σ have a great influence on average consolidation degree. The smaller the intermission parameter β is, the shorter the intermission period of the load is, the more energy the load produces at the same time, which leads to the greater the average consolidation degree. The smaller the loading parameter α is, the longer the trapezoidal cyclic load is in the q_u stage, the more the energy generated by the loading is, and the larger the corresponding average consolidation degree is. Since the loading method in this paper has constant loading, the smaller the N_σ is, the closer the loading form is to the constant load, and the larger the corresponding average consolidation degree is.

(3) For similar projects, it is necessary to estimate the parameters β, α and N_σ of the loading to avoid the safety hazard of the upper structure caused by the large error of parameter selection.

REFERENCES

1 GUAN Shanhai, XIE Kanghe, HU Anfeng. Analysis of one-dimensional consolidation behavior of soils under low-frequency cyclic loading. Rock and Soil Mechanics, 2003, (05): 849-853.

2 Baligh, MM, Levadoux, JN. Consolidation theory for cyclic loading. Journal of the Geotechnical

Engineering Division. 1978;104(4): 415-431.
3 Juran, I, Bernardet, A. La consolidation unidimensionnelle sous charge cyclique. Revue française de géotechnique. 1986(36): 17-30.
4 Favaretti, M, Mazzucato, A, Settlement of a silo subjected to cyclic loading, ASCE, 1994, pp. 775-785.
5 Favaretti, M, Soranzo, M, A simplified consolidation theory in cyclic loading conditions, 1995, pp. 405-409.
6 Rahal, MA, Etude de la consolidation unidimensionnelle d'un kaolin soumis à des chargements par paliers et sinusoïdaux, Rennes, INSA, 1993.
7 Vuez, A, Rahal, A, Cyclic loading for the measuring of soil consolidation parameters, ASCE, 1994, pp. 760-774.
8 Rahal, MA, Vuez, AR. Analysis of settlement and pore pressure induced by cyclic loading of silo. J Geotech Geoenviron. 1998;124(12): 1208-1210.
9 Xie, K, Qi, T, Dong, Y. Nonlinear analytical solution for one-dimensional consolidation of soft soil under cyclic loading. J Zhejiang Univ-Sc a. 2006;7(8): 1358-1364.
10 XIE Kang-he，ZHOU Jin，DONG Yaqin. Analytical solution for one-dimensional nonlinear consolidation of soil under cyclic loadings. Chinese Journal of Rock Mechanics and Engineering, 2006, (01): 21-26.
11 Razouki, SS, Bonnier, P, Datcheva, M, Schanz, T. Analytical solution for 1d consolidation under haversine cyclic loading. Int J Numer Anal Met. 2013;37(14): 2367-2372.
12 SHI Xuchao, LI Hengda. ABAQUS simulation analysis on consolidation of silo buildings foundation in operational period. Journal of Henan University of Urban Construction, 2016, 25(6):4.
13 Cheng Da-wei, Chen Xi. 1D non-linear consolidation under haversine repeated loading. Journal of Chang’an University (Natural Science Edition). 2017;37(5): 8.
14 Indraratna, B, Attya, A, Rujikiatkamjorn, C. Experimental investigation on effectiveness of a vertical drain under cyclic loads. J Geotech Geoenviron. 2009;135(6): 835-839.
15 Indraratna, B, Ni, J, Rujikiatkamjorn, C, Investigation on effectiveness of a prefabricated vertical drain during cyclic loading, IOP Publishing, 2010, pp. 12091.
16 Razouki, SS. Radial consolidation clay behaviour under haversine cyclic load. Proceedings of the Institution of Civil Engineers-Ground Improvement. 2016;169(2): 143-149.
17 Kim, P, Kim, H, Kim, Y, Paek, C, Oh, S, So, S. Nonlinear radial consolidation analysis of soft soil with vertical drains under cyclic loadings. Shock Vib. 2020;2020.
18 JIANG Wenhao， ZHAN Liangtong. Analytical solution for nonlinear consolidation of sand-drained ground considering the time-dependent well resistance. Chinese Journal of Rock Mechanics and Engineering, 2021, 40(01): 187-195.
19 JIANG Wen-hao, ZHAN Liang-tong, YANG Ce, et al. Analytical solution and analysis for consolidation of sand-drained ground considering the time-dependent well resistance and radial-vertical flow. ENGINEERING MECHANICS, 2021, 38(06): 218-226.
20 Lu, M, Wang, S, Sloan, SW, Indraratna, B, Xie, K. Nonlinear radial consolidation of vertical drains under a general time‐variable loading. Int J Numer Anal Met. 2015;39(1): 51-62.
21 CHEN Guohong, XIE Kanghe, CHENG Yongfeng, et al. Analytical solution for consolidation of sand-drained ground considering variation of permeability coefficient in smeared zone. Journal of Zhejiang University (Engineering Science). 2011;45(4): 6.
22 Indraratna, B, Perera, D, Rujikiatkamjorn, C, Kelly, R. Soil disturbance analysis due to vertical drain installation. P I Civil Eng-Geotec. 2015;168(3): 236-246.
23 Nguyen, B, Kim, Y. An analytical solution for consolidation of pvd-installed deposit considering nonlinear distribution of hydraulic conductivity and compressibility. Eng Computation. 2019.

24 ZHAO Dan. Application of tank foundation and water-filling preloaded foundation. Petrochemical Design, 2016, 33(04): 42-45.